applied sciences

MDPI

Article

Characterisation of Microstructure and Mechanical Properties of Linear Friction Welded α+β Titanium Alloy to Nitinol

Ateekh Ur Rehman [1,*], Nagumothu Kishore Babu [2], Mahesh Kumar Talari [2], Yusuf Usmani [1] and Hisham Alkhalefah [3]

[1] Department of Industrial Engineering, College of Engineering, King Saud University, Riyadh 11421, Saudi Arabia; yusmani@ksu.edu.sa

[2] Department of Metallurgical and Materials Engineering, National Institute of Technology, Warangal 506004, India; kishorebabu@nitw.ac.in (N.K.B.); talari@nitw.ac.in (M.K.T.)

[3] Advanced Manufacturing Institute, King Saud University, Riyadh 11421, Saudi Arabia; halkhalefah@ksu.edu.sa

* Correspondence: arehman@ksu.edu.sa

Featured Application: Variable Area Nozzle integrated into the design of a high-bypass-ratio turbofan engine.

Abstract: A variable area nozzle integrated into the design of a high-bypass-ratio turbofan engine effectively saves up to 10% in aircraft fuel consumption. Additionally, noise emissions can be lowered at airports during take-off and landing by having better control of the nozzle diameter. Shape memory capabilities of Nitinol alloys could be availed in the form of actuators in the construction of such a nozzle. However, these Nitinol actuators must be joined to Ti-6Al-4V, a prominent alloy making up most of the rest of the nozzle. Because of the huge differences in the physical and metallurgical properties of these alloys, fusion welding is not as effective as solid-state welding. In the current study, a linear friction welding process was adopted to join Ti-6Al-4V to Nitinol successfully. The effect of friction welding on the evolution of weld macro and microstructures; hardness and tensile properties were studied and discussed. The macrostructure of Ti-6Al-4V and Nitinol's dissimilar joint revealed flash formation mainly on the Ti-6Al-4V side due to its reduced flow strength at high temperatures. Optical microstructures revealed fine grains in Ti-6Al-4V immediately adjacent to the interface due to dynamic recrystallisation and strain hardening effects. In contrast, Nitinol remained mostly unaffected. An intermetallic compound (Ti_2Ni) was seen to have formed at the interface due to the extreme rubbing action, and these adversely influenced the tensile strength and elongation values of the joints.

Keywords: friction welding; Ti-6Al-4V; Nitinol; intermetallic compound; fractography; dissimilar metal joining

Citation: Rehman, A.U.; Kishore Babu, N.; Talari, M.K.; Usmani, Y.; Alkhalefah, H. Characterisation of Microstructure and Mechanical Properties of Linear Friction Welded α+β Titanium Alloy to Nitinol. *Appl. Sci.* **2021**, *11*, 10680. https://doi.org/10.3390/app112210680

Academic Editor: Chaoqun Zhang

Received: 12 October 2021
Accepted: 11 November 2021
Published: 12 November 2021

1. Introduction

Nitinol (equiatomic alloy of nickel (Ni) and titanium (Ti)) alloys are widely used in aerospace, automobile, biomedical, actuators and robotics applications owing to their pseudoelasticity properties, shape memory, excellent corrosion resistance and biocompatibility [1,2]. Titanium and titanium alloys are broadly used in aerospace, marine, chemical, military and medical applications owing to their high strength to weight ratio, excellent corrosion resistance, good fatigue properties and good toughness. α+β titanium alloys are increasing applications in the aerospace and medical fields due to their good corrosion resistance, high specific strength, excellent fracture toughness, and weldability [3–6]. Several aerospace applications, such as a variable area fan nozzle, require Nitinol to be joined with other predominant aerospace alloys such as Ti-6Al-4V.

The welding of Ti and Nitinol alloys is problematic because it readily picks up interstitial elements such as hydrogen, oxygen and nitrogen from the atmospheric gases at high temperatures. An increase in hydrogen, oxygen and nitrogen in the weld metal results in increased strength at the expense of toughness. The melting and solidification of titanium alloys should be carried out in a vacuum or under an inert atmosphere (gas shielding) to avoid these problems. The low thermal conductivities of titanium (17 W/mK) and Nitinol (18 W/mK) leads to longer welding times for high heat input processes like gas tungsten arc welding (GTAW) and gas metal arc welding (GMAW). The long welding time leads to slow cooling and promotes coarse grains in the weld microstructure. In contrast, low heat input processes, such as electron beam welding (EBW) and laser beam welding (LBW), accelerate cooling and promotes fine grains in the weld microstructure [7–10].

Several researchers have attempted to join Nitinol to titanium and its alloys through fusion welding routes, laser welding being the most prominent of those. Despite the fact that laser welding is a highly energy-dense process, the weld pool quality suffered from problems of solidification cracking, non-uniform microstructures and uneven depth of melting between the two base metals. Most notably, it was intermetallics that have rendered the joints extremely brittle [11]. Even when an alloying element such as Nb was added to Nitinol, which ideally should have made the intermetallic formation sluggish, the brittleness of the joint remained the same [12]. When the same Niobium was situated as an interlayer between Nitinol and Ti-6Al-4V, the situation improved. However, the whole welding process had to be precisely controlled, wherein the melting of Nb was carefully avoided by focusing the laser beam more toward one of the base metals [13]. As can be noted, this was more of a design substitute rather than a technological opportunity. The problem of copious amounts of intermetallic formation in laser welding continued to show up in other combinations as well (Nitinol to copper) [14].

Solid-state welding trials showed a few promising results as compared to fusion welding. For instance, diffusion bonding of Nitinol alloy to a titanium alloy, when carried out at the right settings of pressure, temperature and time, produced joints of respectable strength [15]. Even though intermetallics of type Ti_2Ni were seen to have formed in this type of bonding too, the relatively thin nature of such a layer (~40 μm) seems to have a not-so-deleterious effect on the joint strength. When the same interlayer grew thicker (~130 μm), because of higher temperature settings, the strength fell precipitously. Similarly, ultrasonic bonding of Nitinol, another type of solid-state welding, did not yield intermetallics when joined in the presence of a copper interlayer. It has to be noted here that the same copper produced plenteous amounts of intermetallics in laser welding, as discussed in the preceding paragraph. These observations suggest that solid-state joining processes have a better prospect of joining Nitinol to other alloys.

Rehman et al. deployed rotary friction welding, another type of solid-state welding, to join Nitinol to Ti-6Al-4V [16]. The joints showed promising strengths of up to 50% of the base metals' strength. These values were as good as laser and electron beam welds [17,18]. It has to be mentioned here that Niobium had to be used as an interlayer in the mentioned studies of laser and electron beam welding. Direct joints were immensely brittle and failed immediately after the welding. Some of the advantages of friction welding over the beam-based techniques are that highly thicker rods could be joined, and there was no need for a complex joint design. Even though the strength of the joints was appreciably better, the joints still failed in the weld with some brittle features. Ti_2Ni intermetallics were found to be present in the interface.

Linear friction welding (LFW) is a variant of rotary friction welding. Unlike rotary friction welding, the base materials could be in a plate form in linear friction welding. The heat required to join the two materials is generated by back and forth rubbing actions between the base metals. Achieving this oscillatory motion is comparatively difficult from the rotary motion and requires expensive and complex machinery. For this very reason, linear friction welding has become the mainstay in high-end aerospace applications such as BLISK manufacturing [19].

Schematic of Base Plates and Their Setup in the Linear Friction Welding Machine

Linear friction welding consists of four phases, as described initially by Vairis and Frost [20]. In the first stage, when the oscillation of the workpieces begins, the asperities on both surfaces come in close contact. At the same time, heat is generated due to friction. When the conditions are about right—sufficient relative speed and pressure—the heat will soften the materials at the interface. The plasticised material starts to extrude out as a flash. In the subsequent stage, equilibrium conditions are established with regard to the rate of heat generated versus the rate of material extruded. In the final stage, the oscillation is quickly stopped, and an extra pressure called forge pressure is applied on the now stationary workpieces to consolidate the materials into a final joint. The main controllable process parameters are friction pressure, oscillation frequency, amplitude, friction time (all of these during the oscillating) and forge pressure (after the oscillation stops) [9].

In general, heat treatment of a weld improves the joint properties by reducing the residual stresses that might have originated due to the thermal cycles of a welding process. Sometimes, heat treatment is implemented to obtain the desired microstructure in the weld. When it comes to heat treatment of the Nitinol-based weld, one has to be careful not to stimulate the formation of harmful intermetallics. Heat treatment of a Nitinol weld can also alter the alloy's transformation temperature, especially in the region adjacent to the interface. Nevertheless, heat treatment did show positive results when the conditions were just right. Chan et al. [21] showed how with the right post-weld heat treating conditions, one could improve Nitinol laser welds. The authors attributed the improved weld properties to the precipitation of Ni_4Ti_3 during the heat treatment, which arrested the dislocation motion. The benefits of Ni_4Ti_3 were further confirmed by Yan et al. [22]. This time, the Ni_4Ti_3 was reported to benefit the fatigue properties. It has to be noted that the eventual size of the precipitating intermetallics was critical. Only when they were fine (~10 nm) could they become coherent with the matrix and improve the fatigue strength. When the same precipitates were allowed to get bigger—because of higher temperature settings—the properties suffered. Therefore, it could be deduced that lower temperatures, in the range of 350–400 °C, are optimal when heat-treating Nitinol welds. Having said that, not much is known about the effect of heat-treatment on dissimilar welds involving Nitinol, as the literature on this topic is sparse.

As evidenced in the previous paragraphs, fusion [11–14,17,18] and solid-state welding [9,15,16,19,20] techniques were shown to have been quite successful in joining Nitinol to Nitinol, whereas in dissimilar combination welds, Nitinol was poor at bonding with other materials, such as Ti-6Al-4V [11–16]. It has to be noted here that most of these studies concentrated mainly on fusion welding techniques, but not solid-state welding. Rehman et al. [16] were some of the first to employ rotary friction welding to join Nitinol to Ti-6Al-4V. The current study could be considered an extension of that particular study, wherein linear friction welding has been used instead of rotary friction welding. As a matter of fact, linear friction welding is a more suitable joining technique as compared to rotary welding because the joint designs could be of any configuration in linear friction welding, whereas rotary friction welding is restricted to cylindrical configurations only. This study involves welding experiments using linear friction welding to achieve comparatively sound joints and, after that, subject those joints to stress-relieving heat treatment cycles. The joint properties of as-welded joints were compared to the heat-treated ones. Extensive characterisation techniques were used to understand the microstructural changes occurring at the joint interface and how these might influence the overall functional properties of Nitinol were discussed.

2. Materials and Experiment

Ti-6Al-4V and Nitinol in plate form were used for the welding trials. The chemical composition of both the base metals is listed in Table 1. The optical microstructure of Ti-6Al-4V base metal showed primary α grains (white area) elongated in the direction of rolling in a matrix of transformed β (dark area), as shown in Figure 1. The average grain size of Ti-6Al-4V is 67 ± 1 μm. The optical microstructure of Nitinol base metal revealed equiaxed B2 austenite grains, and the average grain size of Nitinol is 50 ±4 μm (Figure 1).

Table 1. Composition of base metals (wt %).

Elements	**Ni**	**Co**	**Cr**	**Fe**	**C**	**N**	**O**	**H**	**Ti**
Ti-6Al-4V	6.01	4.0	0.13	0.03	0.01	0.003	0.112	0.007	balance
Elements	**Ni**	**Co**	**Cr**	**Fe**	**C**	**Nb**	**O**	**H**	**Ti**
Nitinol	55.6	0.005	0.003	0.012	0.03	0.005	0.032	<0.001	balance

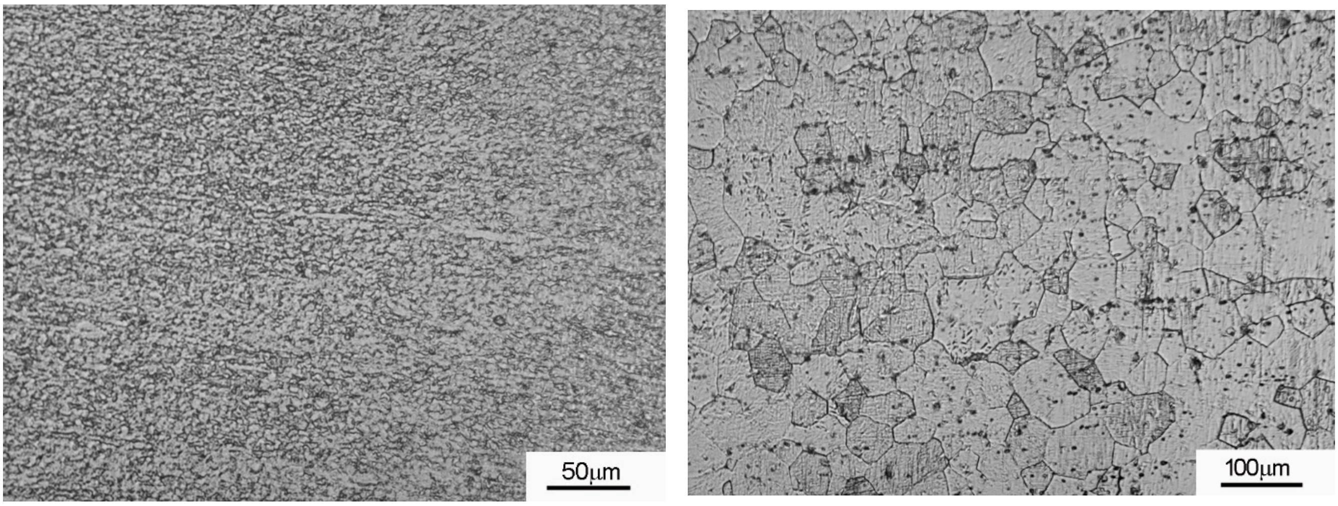

(**a**) (**b**)

Figure 1. Optical microstructures of the base metals: (**a**) Ti-6Al-4V and (**b**) Nitinol.

The dimensions of the plates are shown in Figure 2. A 20 ton linear friction welding machine (Taylor Winfield Technologies Ltd., Youngstown, OH, USA) was employed. Forging force was applied using a hydraulic actuator. The machine had an electro-mechanical oscillation system. The amplitude could go up to a maximum of 6.5 mm. Frequencies between 25 to 60 Hz were possible. The right chuck that holds one of the plates is stationary, whereas the left chuck oscillates at high frequencies to generate the rubbing action. Each plate stuck out from the grips by 4.7 mm.

At the start of the weld cycle, a scrub force of 15 MPa was used in the initial trials. Scrub force helps in cleaning off the surface's contaminants, such as oil and grease. This force also evens out the peaks on the rubbing surfaces. This will go on to help in the subsequent oscillating stage. The trials that used the lower end of the parameters (refer to Table 2) failed to produce satisfactory joints. Therefore, the parameters, especially friction pressure, were raised drastically, which ultimately helped achieve visibly strong joints. Forge pressure seemed to play no significant role, and therefore it was maintained constant throughout the trials. The highly elastic nature of the base metals, especially Nitinol, played a marked role when it comes to the repeatability of the welds: notwithstanding the higher settings, few joints turned out to be defective. This implied that a more rigid fixturing could have remedied the situation to some extent.

The schematic of parent metal plates and their setup in the linear friction welding machine is shown in Figure 2a. The successful weld specimens were sectioned perpendicular to the oscillation direction; in other words, the samples were cut along the Y-direction, as shown in Figure 2b. A typical curve of how the chuck changed its position through a weld cycle is shown in Figure 3. Initially, for some time, the curve remained flat. This was the beginning of the friction stage. The heat built up slowly after the rubbing actions kicked in. After a while, when enough heat was generated, the base metals became plastically soft and started to extrude at a higher rate—meaning the chuck moved rapidly within a small amount of time. However, as the base metals became fully plastic at the interface, they could not generate frictional heat any further, thus entering into the last stage of the weld cycle, where a kind of equilibrium condition set in. In this stage, the slope of the curve flattened out gradually.

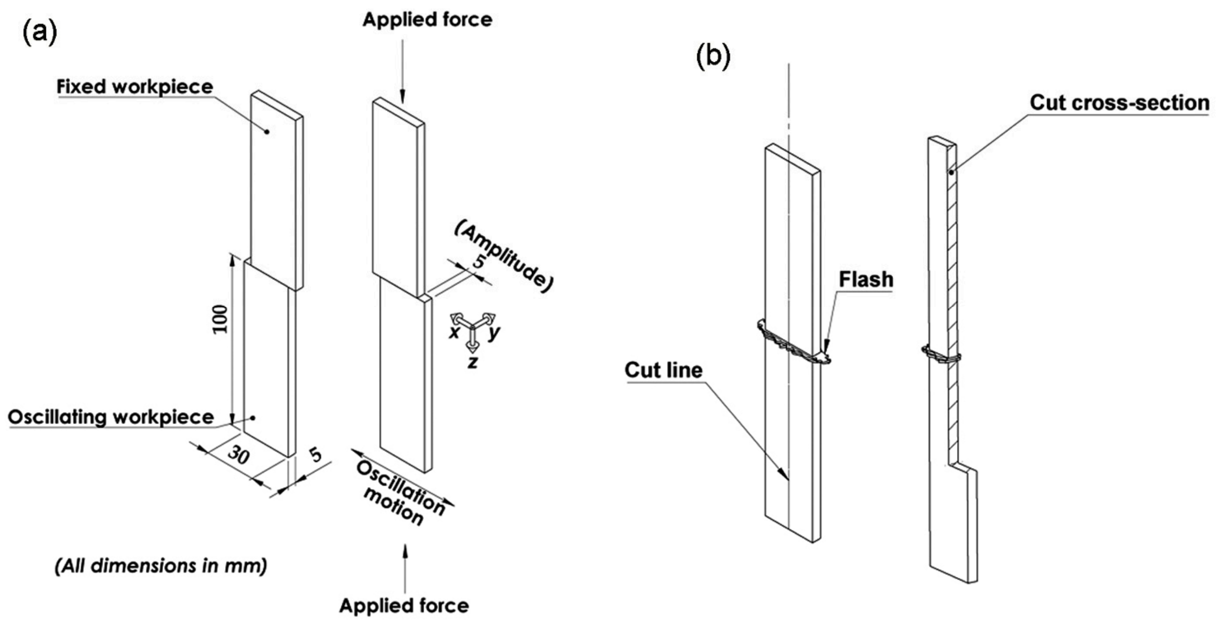

Figure 2. (**a**) Schematic of base plates and their setup in the linear friction welding machine. (**b**) Schematic of the metallographic sample cut away from the welded coupons.

Table 2. Welding parameters.

Parameter	Final Chosen
Friction Pressure (MPa)	190
Forge Pressure (MPa)	110
Amplitude (mm)	5
Frequency (Hz)	60
Burn-off length (mm)	3 mm
Forge time (s)	2 s

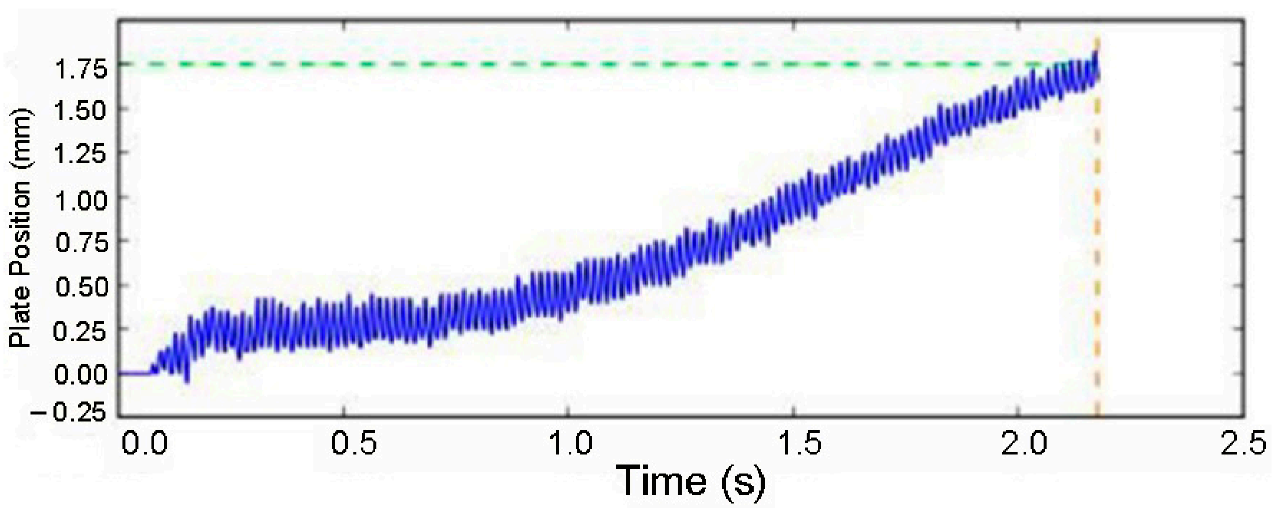

Figure 3. Loss of length in the base plates in the form of a flash in a typical weld cycle.

Linear friction welded specimens were subjected to a PWHT at 400 °C (well below the β transus of the alloy) in a vacuum furnace for an hour, and furnace cooled to room temperature. The dissimilar Ti-6Al-4V/Nitinol linear friction welded specimens in the as-welded and PWHTed conditions were sectioned in the transverse direction to the weld and polished for metallographic study. For microstructure examination of the Ti-6Al-4V side, a solution consisting of a mixture of 2% HF and 3% HNO_3 in 95% distilled water was used, and 40% HNO_3 and 10% HF in 50% distilled water was used for etching on the Nitinol side. The nominal compositions of the base metals were analysed using LECO TCH 400 instrument (LECO Corporation, St. Joseph, MI, USA). The etched samples were observed under a Nikon SMZ745T stereomicroscope (Nikon Instruments Inc., New York, NY, USA) to capture the macrostructure of the weld. Microstructural features of base metals and welds were analysed by Leitz optical microscope (Leitz GMBH & CO. KG, Leitzstrasse 2, Oberkochen, Germany). The microstructure of the welds and fracture surfaces of tensile tested specimens were examined in a scanning electron microscope (VEGA 3LMV, TESCAN ORSAY HOLDING, Brno, Czech Republic), equipped with an Oxford energy dispersive X-ray spectrometer (EDS) (Oxford instruments, TubneyWoods, Abingdon, UK) for line scanning. The welds were subjected to X-ray diffraction (XRD) on PANalytical (Malvern, UK, X'pert powder XRD) using copper Kα radiation to identify various phases in the weld region and base metal.

Microhardness measurements were conducted according to ASTM E384 standard (West Conshohocken, PA, USA) across the weld region at intervals of 0.25 mm at 500 gm load for 15 s on as-welded and PWHT conditions using a Vickers hardness tester (MMT-X Matsuzawa, Akita Prefecture, Kawabetoshima, Japan) equipped with a diamond pyramid indenter. For tensile testing, sub-sized transverse weld specimens with a gauge length of 25 mm, gauge width of 6 mm and thickness of 5 mm were fabricated from linear friction welded samples. Tensile tests for base metals as well as welds were carried out on a Universal Testing Machine (Jinan WDW-100S, Jinan, China) according to ASTM E8 standard at a cross speed of 0.5 mm/min.

3. Results and Discussion

3.1. Macrostructure

Defects such as cracks, solidification cracking and incomplete bonding were not observed upon visual inspection (Figure 4). Flash was seen on all sides of the interface. Nevertheless, the shape was not uniform all around. The flash projected more on the top side than the bottom in Figure 5. This indicates that there was a slightly non-symmetrical situation during the oscillating stage. Either the center lines of the specimen did not align perfectly, or the oscillation mechanism itself was biased more towards one side. Vairis and Frost suggested even minor misalignments between the base metal plates could lead to perceptible changes in the way a flash emerges [20]. Even a minor disturbance in the initial stages will first affect the distribution of the temperature, which leads to a non-uniform material extrusion, and this, in turn, affects the temperature profile, thus settling down into a cause-and-effect loop.

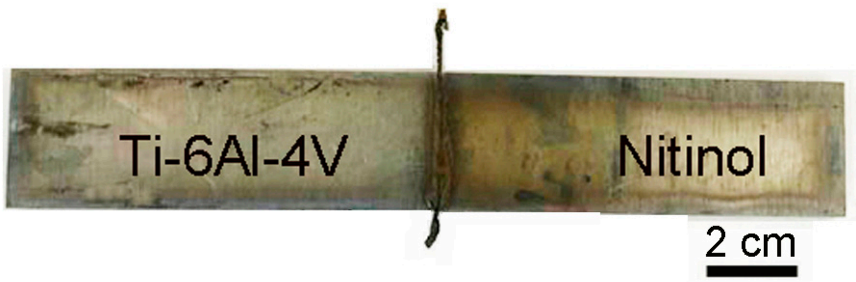

Figure 4. A successfully bonded Ti-6Al-4V/Nitinol dissimilar linear friction weld.

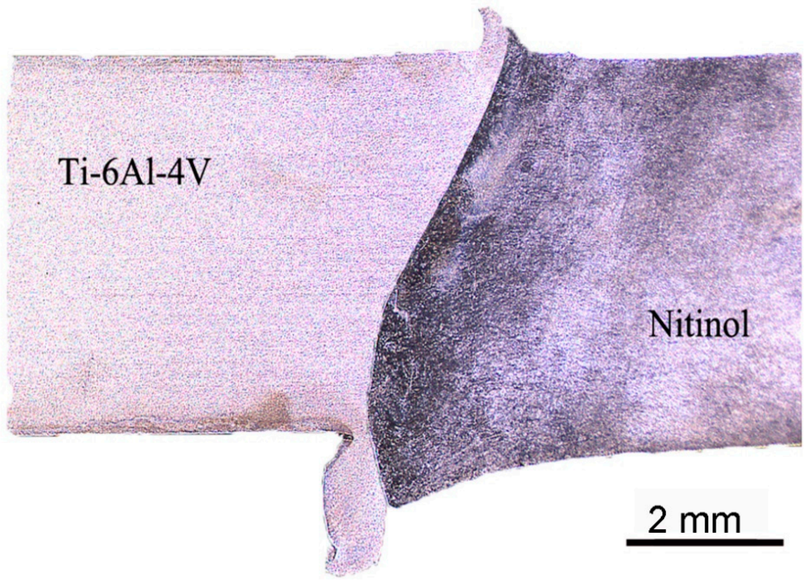

Figure 5. Macrostructure of the dissimilar linear friction welded Ti-6Al-4V/Nitinol sample showing more flash on the Ti-6Al-4V side.

Two mechanisms play a role in the flash formation during friction welding [23]. The first one is because of the oscillation motion between the workpieces: the material is transported from the interiors to the exterior. The material then piles up more at the edges (along the oscillating direction) than at the centre. The second mechanism that influences flash formation is the forging pressure. This is the pressure applied across the cross-sectional area of the weld. The forging pressure pushes material outward more in the central region than at the edges, opposite to what was seen in the first mechanism. For the above reasons, it can be said that the geometry of the flash differs for different weld settings.

The shape of the flash was not uniform along its length. For instance, the outermost edge of the flash was seen to have ridges, whereas the root seemed to be smoother. At the beginning of the weld cycle, when the equilibrium conditions were yet to be established, the base metals would not have become sufficiently soft because the temperature were not high enough. This would be the time when the flash had ridged edges. As the friction stage progressed, a continuous supply of fully plasticised material ensured that the subsequent flash was smoother.

The extent to which Ti-6Al-4V and Nitinol deform as flash (Figure 5) depends upon their yield strength at elevated temperatures. The formation of more flash on the Ti-6Al-4V side and little flash on Nitinol side can be attributed to drop-in flow stresses of Ti-6Al-4V at high temperatures. In addition to this, the poor heat conducting properties of Ti-6Al-4V cause the temperature to rise quickly on its side of the joint. The preferential deformation of one alloy over the other gives rise to the problem of insufficiently cleaned surfaces. One of the advantages of friction welding is its less stringent requirements of the joining surfaces. The rubbing action and the subsequent flash expulsion ensures the impurities, such as oxide films and contaminants, on the surfaces get pushed out, and therefore only virgin surfaces come into contact with each other, ultimately ending up with a strong weld. However, this idealistic scenario breakdown when two materials with different flow properties are brought together. Lack of flow, manifested by material on one side, hinders the much-desired cleaning action. Nevertheless, in the present case, Nitinol has also deformed to some extent (Figure 6), allaying the self-cleaning concern more or less. The same phenomena have been observed during rotary friction welding of dissimilar welds, namely titanium to stainless steel [24] and titanium to Nitinol [16].

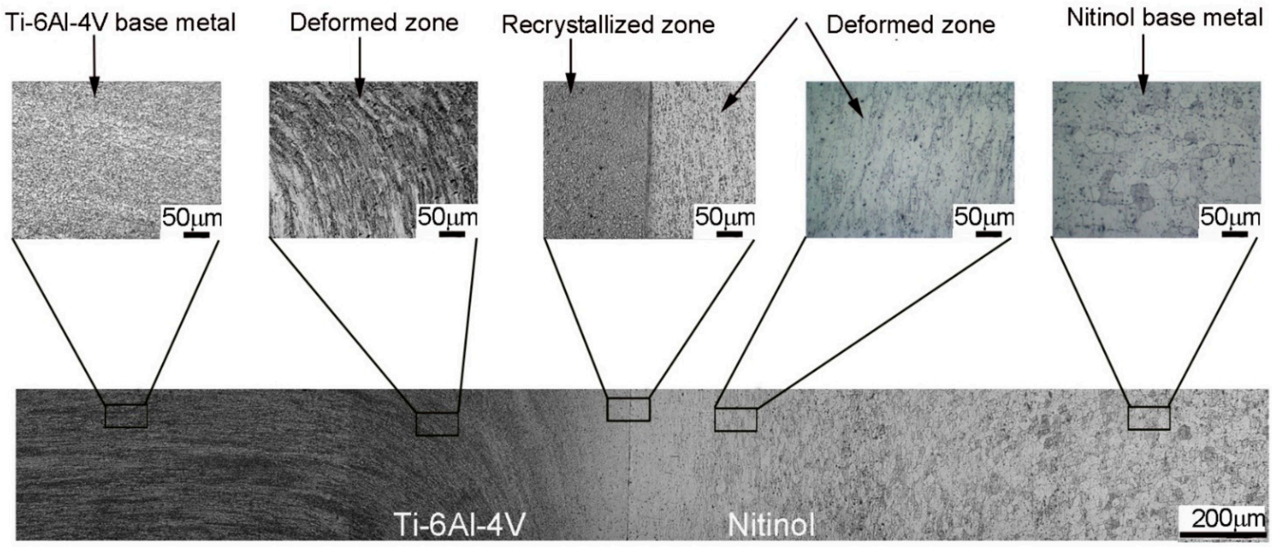

Figure 6. The optical microstructure of the Ti-6Al-4V/Nitinol linear friction welds in the as-welded condition.

In Figure 5, a greater volume of material was seen on one side (bottom) than the other. Since the direction of oscillation is along with the interface (along the plane of the paper), it can be deduced that the base metals were not secured exactly along their central planes. Possibly, the holding fixtures in the machine were slightly off. The weld interface also appeared to be wavy. This waviness is caused by the increase and decrease in temperature with each oscillation. When the temperatures reach higher values at a particular location, the material flows easily for a fraction of a second but immediately hardens up when the temperature falls. Such temperature rises and falls in each cycle of oscillation set a stage for an uneven flash formation.

3.2. Microstructure

The optical microstructure of the Ti-6Al-4V/Nitinol linear friction as-welded joint on the Ti-6Al-4V side showing three distinct zones, namely the recrystallised zone, deformed zone and base metal zones, of Ti-6Al-4V are as shown in Figure 6. In contrast, the deformed zone and base metal of Nitinol were observed on the Nitinol side. The recrystallised zone was observed adjacent to the weld interface on the Ti-6Al-4V side, which is distinguished from all other regions by its whitish appearance at low magnification. The fine grains were observed at high magnification nearer to the weld interface on the Ti-6Al-4V side due to grain refinement induced by dynamic recrystallisation [25]. During dynamic recrystallisation, the material experiences a significant amount of plastic deformation throughout the linear friction welding process. The base metal's low-angle grain boundaries are replaced by high-angle boundaries in the recrystallised zone by means of oscillation during LFW. The fine nuclei of grains begin to develop, eventually forming a microstructure with fine equiaxed grains in the recrystallised zone [25]. Adjacent to the recrystallised zone, there was a deformed zone which is characterised by a highly deformed structure. The base metal Ti-6Al-4V grains were deformed in an upward flowing pattern showing curved, elongated grains in the deformed zone. The deformed zone undergoes plastic deformation, and in this region, no recrystallisation occurs due to insufficient strain. There is a significant deformed zone adjacent to the Nitinol interface, and the microstructure mainly consists of austenite rather than martensite because of the heating of the material during LFW. Microstructural features present in the deformed zone of the Nitinol side show elongated grains when compared to the Nitinol base metal exhibited fine equiaxed grains.

The optical microstructure of Ti-6Al-4V/Nitinol linear friction welds in the post-weld heat-treated condition (PWHT) is shown in Figure 7. It can be observed from Figure 8 that the welds prepared with PWHT at 400 °C showed similar microstructural features compared with the as-welded condition except for some dark regions (etch pits) observed on the Nitinol side. These etch pits have developed during the metallographic etching process. PWHT at 400 °C, below the beta-transus temperature, results in a duplex microstructure of primary α, and transformed β is generated due to slow cooling. Rapid quenching leads to a martensitic transformation of β, resulting in a very fine needle-like microstructure [3]. However, in the present study, rapid cooling is not employed during PWHT at 400 °C, leading to equiaxed α in a β matrix. From the optical micrographs, it is difficult to identify the phases and intermetallics present in the microstructure; therefore, further work by XRD is necessary.

The SEM images (refer below Figure 8a,b) showed a continuous region of intermediate phases at the interface. This region seems to be around 10 μm thick. This region could easily have consisted of the oxides of Ti and Ni [26]. Elemental Ti and Ni from both the base metals, which are present majorly composition-wise, would react with the oxygen present on the surfaces during the friction stage. It has to be noted that previous works on friction welding suggest that the chance of this happening—oxygen reacting with the base metal elements—is quite low [27,28]. This is because the friction stage is very short, and also even if some oxide phases do form, they eventually were pushed out as flash. This reasoning might be valid to a large extent for rotary friction welding, but not so in the case of linear friction welding. One of the drawbacks of linear friction welding compared to rotary friction welding is, while oscillating, the base metal rubbing surfaces—hot as they are—will be exposed to ambient conditions, even if that were for a fraction of a second [29]. This is when oxides would form. The greater the amplitude, the higher the chances of oxide formation. This is not seen in rotary friction welding, wherein the hot metal is always shielded from the ambient air.

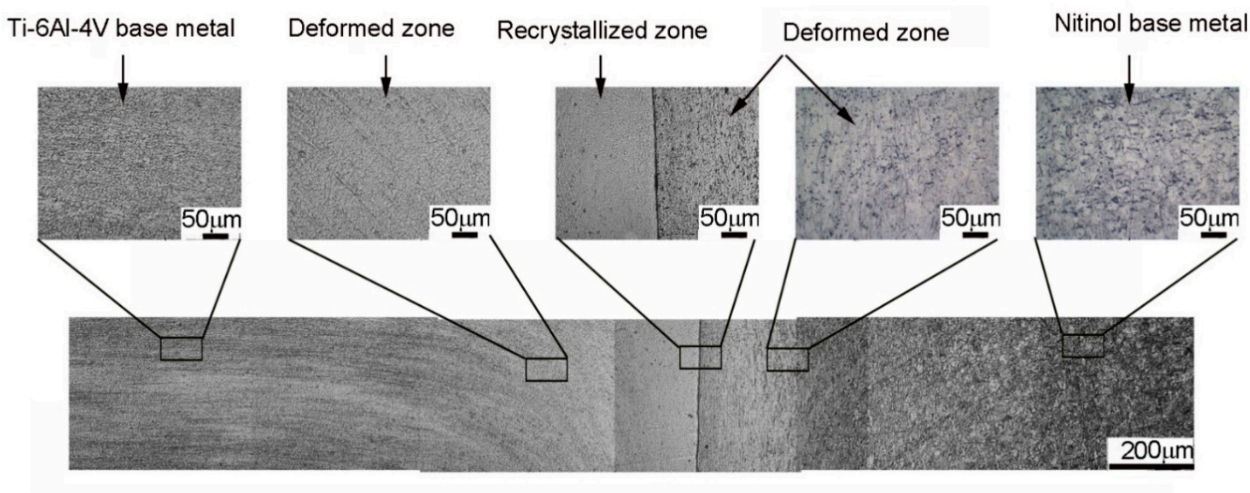

Figure 7. The optical microstructure of the Ti-6Al-4V/Nitinol linear friction welds in the post-weld, heat-treated (PWHT) condition.

In addition to oxides, it is possible for chemical elements such as Ni and Ti to have formed intermetallics between themselves. During the friction stage, when there are higher temperatures present and the materials are under severely plasticised conditions, it is highly possible that there is a mechanical intermixing of the elements as well as the diffusion of these elements across the interface. Figure 8a shows that there is a sudden compositional change at the interface. This suggests that Ni and Ti would have formed intermetallic phases. According to the phase diagram, $NiTi_2$ and Ni_3Ti are the most prominent phases that would result if Ni and Ti were brought together at high temperatures. In the line scan, it is seen that the percentage of Ti is higher whether it is on the Ti-6Al-4V side or the Nitinol side; the chance of formation of Ti-rich $NiTi_2$ is higher. The microstructural analysis (Section 3.3) suggested that it was Ti-6Al-4V that deformed more. So, it is highly likely that the phases formed at the interface were rich in Ti rather than Ni. Since $NiTi_2$ is a highly brittle compound [30], its presence in the welds indicates the possibility of a brittle joint.

Nevertheless, since the thickness of this intermixed zone is quite low (~10 μm), its effect would be subdued on the joint strength.

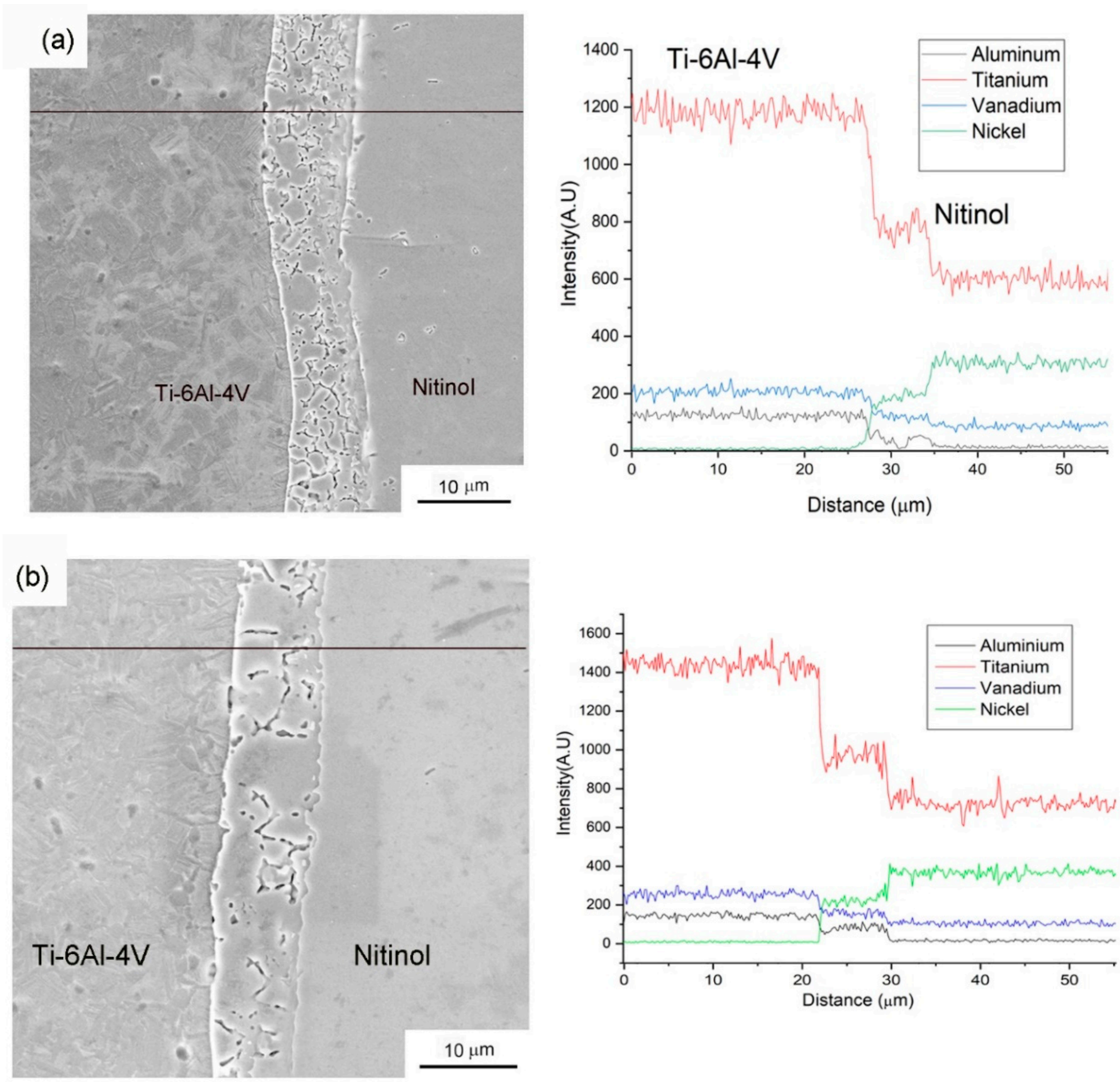

Figure 8. Scanning electron microscopy image in secondary electron mode showing (**a**) Ti-6Al-4V/Nitinol weld interface in the as-welded condition (left) and the corresponding energy dispersive spectroscopy (EDS) line scan. (**b**) Ti-6Al-4V/Nitinol weld interface after heat treatment (left) and the corresponding energy dispersive spectroscopy (EDS) line scan.

Figure 8b shows the same interface after PWHT. It is not clear from the line scan if there were any chemical compositional changes, but at least there was no sign of a major thickness increase. This means the joint strength should remain more or less the same. The structure of the intermediate zone could be seen to have a grain-based microstructure. Before PWHT, the grain structure was finer, whereas, after PWHT, the grains became broader. It looks like even though PWHT has not altered the overall chemical composition nor the thickness of the zone, it surely has affected the grain morphology of the intermediate zone. It is highly possible that the intermetallic zone consisted of Ti_2Ni as suggested by the EDS line scan. Ti_2Ni was seen to form readily in the laser weld of Ti64 and NiTi [31].

The X-ray diffraction (XRD) patterns of the Ti-6Al-4V parent metal and Nitinol parent metal are presented in Figure 9. This also shows the tensile fracture surface of the Ti-6Al-4V/Nitinol linear friction welds in the as-welded and PWHT conditions. XRD analysis of the Ti-6Al-4V base metal revealed the presence of the hexagonal α phase along with the β phase, while Nitinol base metal showed the austenitic (B2-cubic) phase in the microstructure. In contrast to the base metals, the fracture surface of the Ti-6Al-4V/Nitinol linear friction welds in the as-welded and PWHT conditions showed a hexagonal α phase and the presence of a Ti_2Ni intermetallic phase. It can be seen from Figure 9 that the PWHT does not alter the phase constitution of the as-welded sample. A slight increase in the Ti_2Ni intermetallic phase diffraction peak intensity was observed after the PWHT. Chan et al. reported that the PWHT of similar Nitinol–Nitinol Laster weds at 400 °C and 500 °C (1 h holding time) resulted in the formation of metastable Ti_3Ni_4 precipitates [21]. However, the intermixing zone of as-welded and PWHT friction welded joints in this study were rich in titanium, thus forming the titanium-rich intermetallics (Ti_2Ni). It was reported that the formation of Ti_2Ni intermetallic phases in the welded joint is influenced mainly by welding parameters and the base metal chemical composition [16].

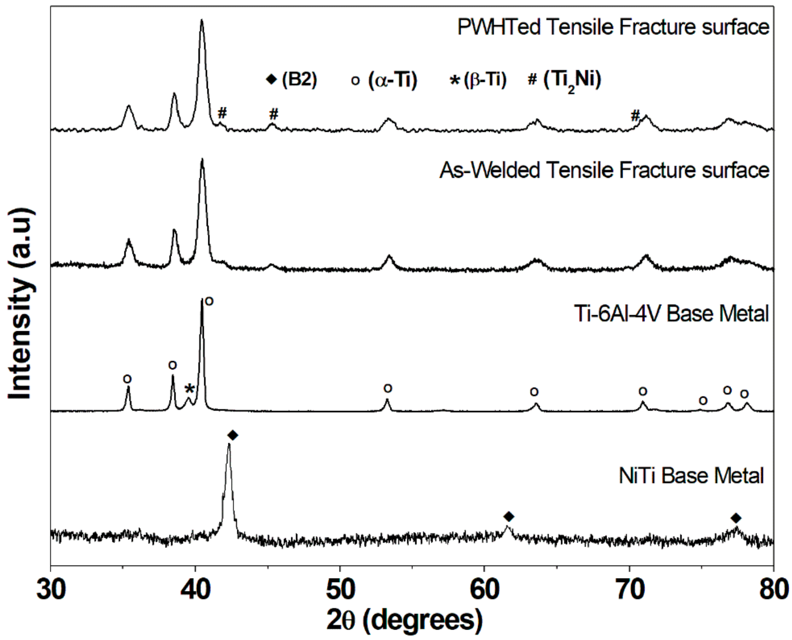

Figure 9. X-ray diffraction (XRD) profiles of the Ti-6Al-4V base metal, Nitinol base metal and fracture surface of the LFW welds in the as-welded and PWHT conditions.

3.3. Mechanical Properties

3.3.1. Hardness

Microhardness distribution across the interface of dissimilar Ti-6Al-4V/Nitinol linear friction welds in the as-welded and PWHT conditions is shown in Figure 10. A higher value of microhardness (371–379 HV) in the as-welded joint just adjacent to the Ti-6Al-4V side can be attributed to strain hardening that occurred during the linear friction welding process. In contrast, a slight reduction in hardness (349–357 HV) after PWHT on the Ti-6Al-4V side and was attributed to the reduction in residual stresses. However, a decrease in hardness on the Nitinol side was attributed to a limited amount of deformation. Similar observations are obtained during rotary friction welding of titanium to stainless steel joints [24]. On the Nitinol side, a slight increase in hardness distribution (264–267 HV) in the deformed zone of the as-welded condition when compared to the PWHT condition (254–257 HV) from the weld interface to the base metal is noticed. For the hardness (344–367 HV) of Ti-6Al-4V base metal, it is also observed that it is higher than Nitinol (232–245 HV). There was no significant difference in hardness values among the base metals in the as-welded and PWHT conditions. The highest hardness observed at the Ti-6Al-4V/Nitinol weld interface of as-welded and PWHT conditions may be attributed to the formation of intermetallics of Ti and Ni, such as Ti_2Ni, conformed by XRD analysis.

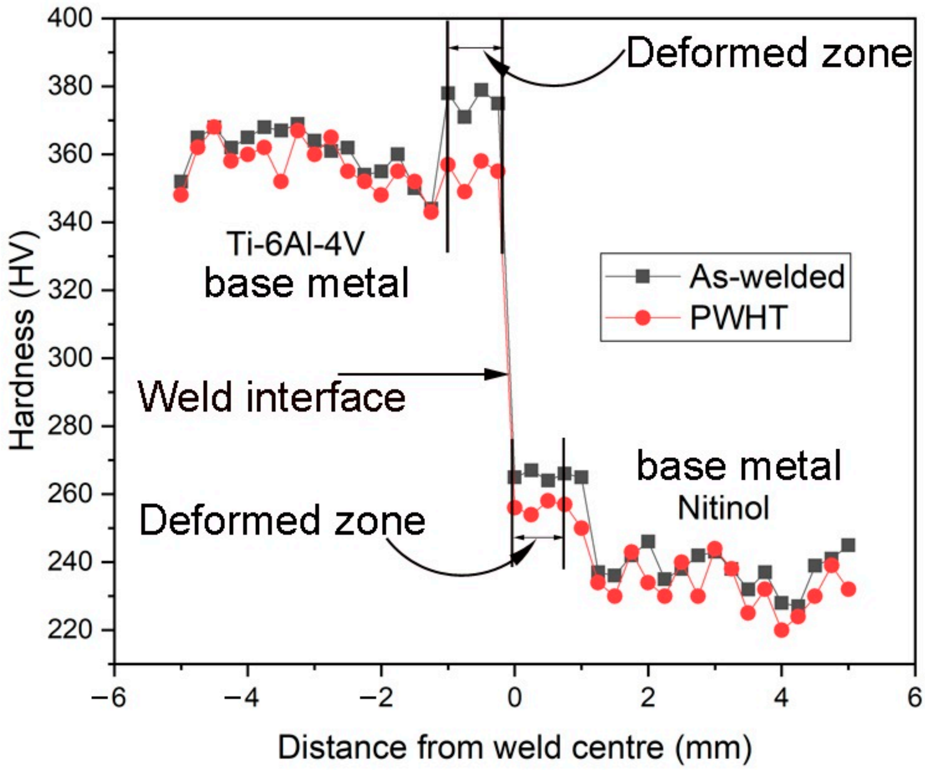

Figure 10. Hardness distribution across the interface of dissimilar Ti-6Al-4V/Nitinol linear friction welds in the as-welded and PWHT conditions.

3.3.2. Tensile Properties

Tensile tests were conducted for the dissimilar Ti-6Al-4V/Nitinol joints in the as-welded and PWHT conditions. The tensile plots are shown in Figure 11. The base metal tensile curves have been included in Figure 11 for comparison. Three samples of each were tested. The dissimilar weldments in the as-welded and PWHT conditions exhibited lower strength and ductility values compared with the wrought base metals (Ti-6Al-4V: UTS = 1065 MPa, 15% elongation; Nitinol: UTS = 883 MPa, 17% elongation). This could be attributed to the formation of intermetallics of Ti and Ni, such as Ti_2Ni at the weld interface. As discussed earlier, the XRD data of the fracture surface showed the presence of Ti_2Ni intermetallic phase in the as-welded and PWHT conditions (Figure 9).

The dissimilar Ti-6Al-4V/Nitinol linear friction welded joint exhibited a slightly higher ultimate tensile strength (UTS) and lower ductility (UTS = 282 MPa, 3.9% elongation) compared with PWHT condition ((UTS = 250 MPa, 5.9% elongation). The presence of the strain hardening effect at the weldment could be the reason for the higher strength in the as-welded condition. However, PWHT could result in a reduction in strain energy and cause a slight decrease in the strength of the weldment. Further, the improvement of the weld ductility in the PWHT condition, compared to the as-welded condition, could also be attributed to the reduction in residual stress and strain energy. PWHT was found to have significantly improved the tensile strength and fracture elongation in similar joints of Nitinol [21]. When the PWHT temperature was just about right (350 °C), the tensile strength went up to 550 MPa from about 500 MPa (as-welded condition). Any further increase in the PWHT affected the weld properties negatively. This kind of behaviour is in line with the results seen in the current work.

The strength values in the current study (282 MPa) are a little below the values reported by Zoeram et al. [31] (300 MPa) and Zhan et al. [13] (480 MPa). Nevertheless, it has to be remembered that both of these studies incorporated a third material, such as Cu and Nb, to stop intermixing of the Ti and Ni. In both studies, direct joints (without filler material) failed immediately after welding. Joints that involve a third alloy might create challenges such as galvanic corrosion. Therefore, whenever a direct joint between Ti-6Al-4V and Nitinol is desired, the current study results show a promise that linear friction welding might be a better route compared to fusion ones.

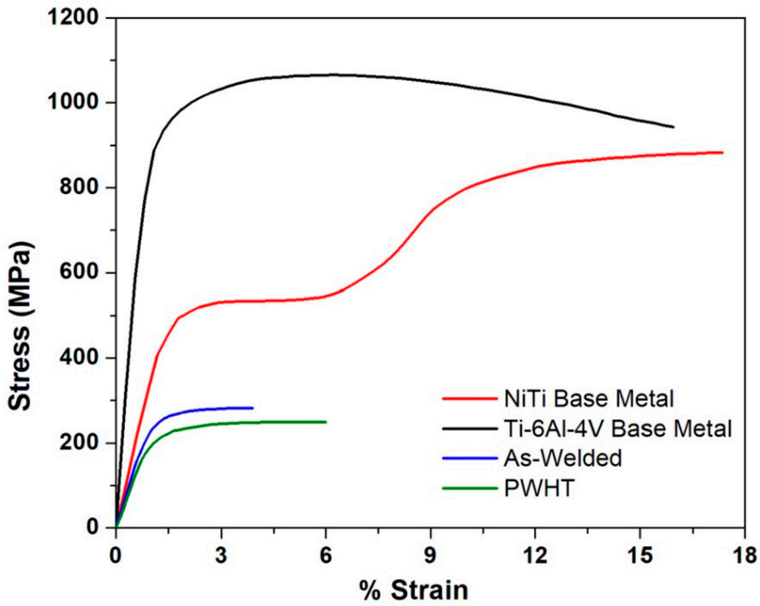

Figure 11. The typical tensile properties of base metals and dissimilar Ti-6Al-4V/Nitinol friction linear friction welds in the as-welded and PWHT conditions.

The dissimilar Ti-6Al-4V/Nitinol joints in the as-welded and PWHT conditions failed at the weld interface after tensile testing, as shown in Figure 12a,b, respectively. According to XRD patterns, the fracture surface of dissimilar Ti-6Al-4V/Nitinol welds in the as-welded and PWHT conditions contains Ti_2Ni intermetallic phase at the weld interface. This could be the main reason for the failure of welds at the weld interface in both conditions. Upon tensile testing, the deformation of the weld is restricted due to the early cracking of the Ti_2Ni intermetallic phase. Further, mechanical constraint provided by the relatively non-deforming Ti-6Al-4V and Nitinol base metals at the stresses of consideration restricts the deformation of the weld interface region [32]. Hence, this constraint at the weld interface results in the triaxial state of the stresses at the weld interface and reduces the deformation tendency. As a result, fracture occurs at the weld interface, which is the weakest part of the weld joint

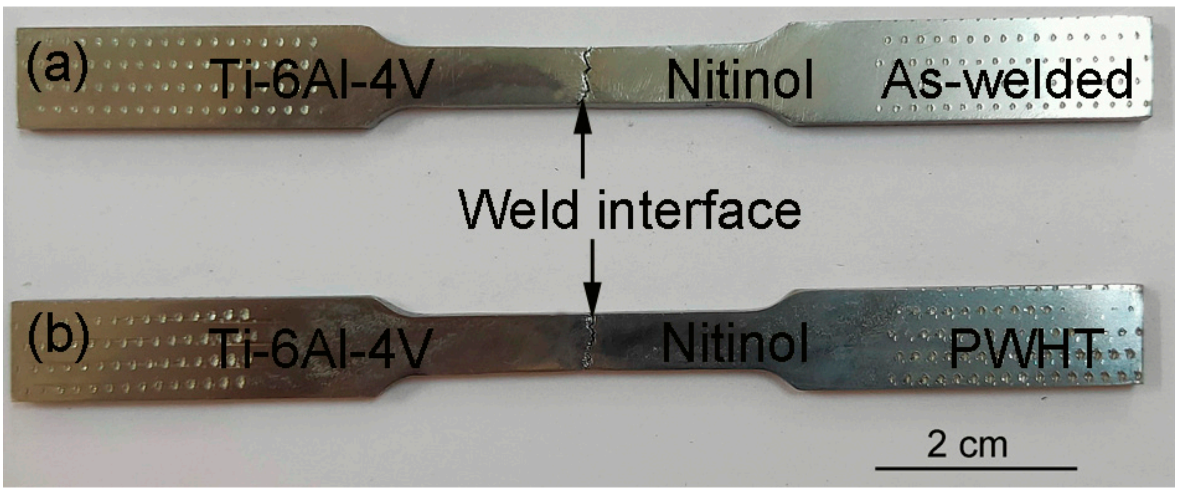

Figure 12. The failure location of the dissimilar Ti-6Al-4V/Nitinol joints in the (**a**) as-welded and (**b**) PWHT conditions.

The fractographs of the failed surface of Ti-6Al-4V in the as-welded and PWHT conditions are shown in Figure 13a,b, respectively. The results in Figure 13 suggest that fracture occurred by a cleavage mode of fracture, which indicates that the specimen fails in a brittle manner under the action of tensile testing in both conditions.

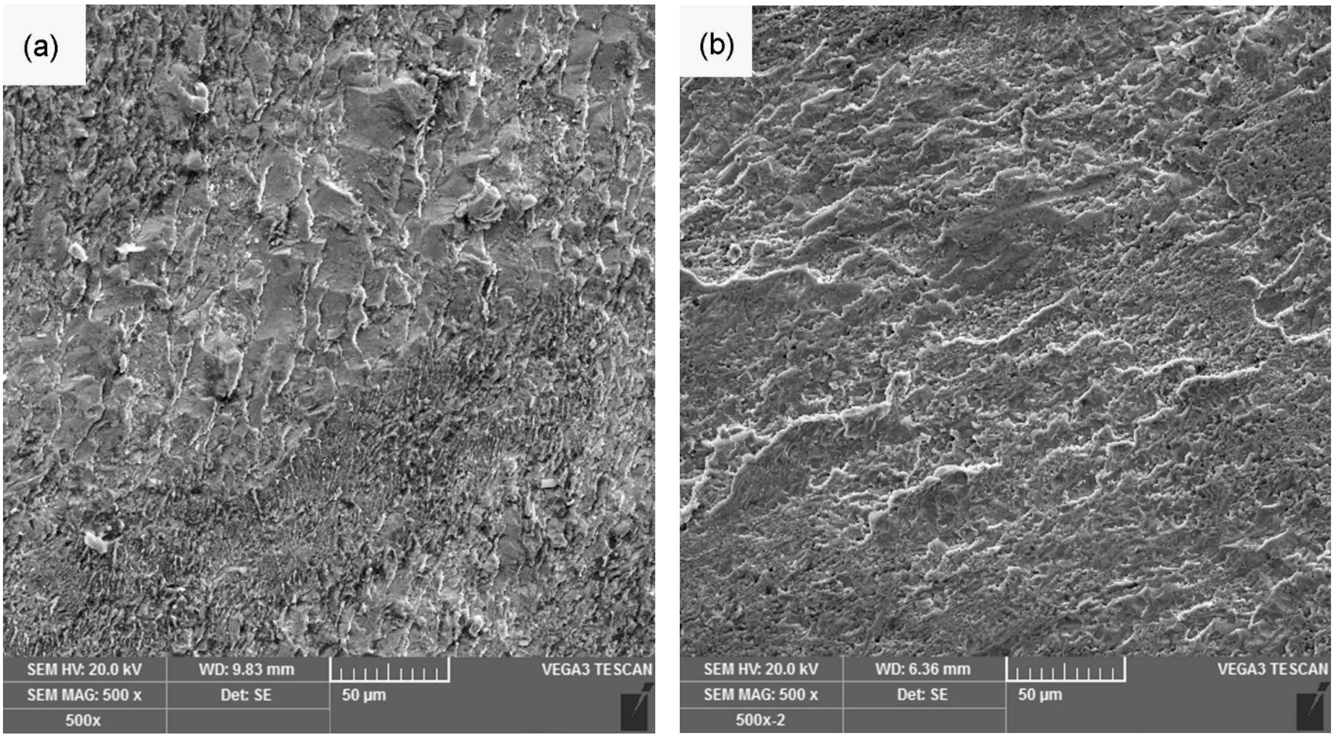

Figure 13. Fracture surfaces of the dissimilar Ti-6Al-4V/Nitinol welded joints in the (**a**) as-welded and (**b**) PWHT conditions.

4. Conclusions

In the present study, the dissimilar Ti-6Al-4V/Nitinol welds were prepared using the linear friction welding technique. The influence of macrostructure and microstructure on hardness and tensile properties were investigated for dissimilar Ti-6Al-4V/Nitinol as-welded and PWHT conditions. The following conclusions were drawn.

- A defect-free dissimilar Ti-6Al-4V/Nitinol weld (no cracks, solidification cracking, incomplete bonding) could be obtained by a linear friction welding technique.
- The macrostructure of dissimilar Ti-6Al-4V/Nitinol welds exhibited more flash on the Ti-6Al-4V side, and little flash on Nitinol side can be attributed to drop-in flow stresses of Ti-6Al-4V at high temperatures.
- X-ray diffraction studies revealed a formation of titanium-rich intermetallics (Ti_2Ni) on the fracture surface of linear friction welds in the as-welded and PWHT conditions. This could be attributed to the diffusion of Ti being higher at the weld interface than Ni.
- The dissimilar Ti-6Al-4V/Nitinol linear friction welded joint exhibited a slightly higher ultimate tensile strength (UTS) and low ductility (UTS = 282 MPa, 3.9% elongation) compared with PWHT condition (UTS = 250 MPa, 5.9% elongation), and this may be attributed to high residual stresses in the as-welded condition and Ti_2Ni brittle intermetallics present at the weld interface.
- The tensile fracture surfaces of the dissimilar Ti-6Al-4V/Nitinol linear friction welds exhibited cleavage (brittle) mode of fracture due to the formation of Ti_2Ni intermetallics at the weld interface.

Author Contributions: Conceptualisation, A.U.R., Y.U. and H.A.; methodology, A.U.R., N.K.B., M.K.T. and Y.U.; formal analysis, A.U.R., N.K.B., M.K.T., Y.U. and H.A.; investigation, A.U.R., N.K.B., M.K.T. and Y.U.; resources, A.U.R., Y.U and H.A.; data curation, A.U.R., N.K.B. and M.K.T.; writing—original draft preparation, A.U.R., N.K.B. and M.K.T.; writing—review and editing, A.U.R., N.K.B., M.K.T., Y.U. and H.A.; visualisation, A.U.R., N.K.B. and M.K.T.; supervision, A.U.R., N.K.B. and M.K.T.; project administration, A.U.R. and Y.U.; funding acquisition, A.U.R., Y.U. and H.A. All authors have read and agreed to the published version of the manuscript.

Funding: National Plan for Science, Technology and Innovation (MAARIFAH), King Abdulaziz City for Science and Technology, Kingdom of Saudi Arabia, Award Number (14-ADV110-02).

Institutional Review Board Statement: Not Applicable.

Informed Consent Statement: Not Applicable.

Data Availability Statement: Data are contained within this article.

Acknowledgments: This project was funded by the National Plan for Science, Technology and Innovation (MAARIFAH), King Abdulaziz City for Science and Technology, Kingdom of Saudi Arabia, Award Number (14-ADV110-02).

Conflicts of Interest: The authors declare no conflict of interest.

References

1. Jani, J.M.; Leary, M.; Subic, A.; Gibson, M.A. A Review of Shape Memory Alloy Research, Applications and Opportunities. *Mater. Des.* **2014**, *56*, 1078–1113. [CrossRef]
2. Saedi, S.; Turabi, A.S.; Andani, M.T.; Moghaddam, N.S.; Elahinia, M.; Karaca, H.E. Texture, aging, and superelasticity of selective laser melting fabricated Ni-rich NiTi alloys. *Mater. Sci. Eng. A* **2017**, *686*, 1–10. [CrossRef]
3. Boyer, R.R. Titanium and titanium alloys. In *Metals Handbook*; Davis, J.R., Ed.; ASM International: Materials Park, OH, USA, 1998; pp. 575–588. ISBN 978-0-87170-654-6.
4. Niinomi, M. Mechanical properties of biomedical titanium alloys. *Mater. Sci. Eng. A* **1998**, *243*, 231–236. [CrossRef]
5. Gurrappa, I. Characterization of titanium alloy Ti-6Al-4V for chemical, marine and industrial applications. *Mater. Charact.* **2003**, *51*, 131–139. [CrossRef]
6. Sidambe, A. Biocompatibility of Advanced Manufactured Titanium Implants—A Review. *Materials* **2014**, *7*, 8168–8188. [CrossRef] [PubMed]
7. Gould, J.E.; Baselack, W.A., III; Williams, J.C. Some aspects of welding on the structure and properties of titanium alloys. In *Advanced Processing Methods for Titanium*; Hasson, D.F., Hamilton, C.H., Eds.; The Metallurgical Society of AIME: Warrendale, PA, USA, 1982; pp. 203–223.
8. Babu, N.K.; Raman, S.G.S.; Murthy, C.V.S.; Reddy, G.M. Influence of beam oscillation patterns on the structure and mechanical properties of Ti–6Al–4V electron beam weldments. *Sci. Technol. Weld. Join.* **2005**, *10*, 583–590. [CrossRef]
9. Dalgaard, E.; Wanjara, P.; Gholipour, J.; Cao, X.; Jonas, J.J. Linear friction welding of a near-b titanium alloy. *Acta Mater.* **2012**, *60*, 770–780. [CrossRef]
10. Gupta, B.; Pandey, S.; Nahata, A.; Zhang, T.; Nahata, A. Bistable physical geometries for terahertz plasmonic structures using shape memory alloys. *Adv. Opt. Mater.* **2017**, *5*, 1601008. [CrossRef]
11. Datta, S.; Raza, M.S.; Kumar, S.; Saha, P. Exploring the possibility of dissimilar welding of NiTi to Ti using Yb-fiber laser. *Adv. Mater. Process. Technol.* **2018**, *4*, 614–625. [CrossRef]
12. Yuhua, C.; Yuqing, M.; Weiwei, L.; Peng, H. Investigation of welding crack in micro laser welded NiTiNb shape memory alloy and Ti6Al4V alloy dissimilar metals joint. *Opt. Laser Technol.* **2017**, *91*, 197–202. [CrossRef]
13. Oliveira, J.P.; Panton, B.; Zeng, Z.; Andrei, C.M.; Zhou, Y.; Miranda, R.M.; Braz Fernandes, F.M. Laser joining of NiTi to Ti6Al4V using a Niobium interlayer. *Acta Mater.* **2016**, *105*, 9–15. [CrossRef]
14. Zeng, Z.; Oliveira, J.P.; Yang, M.; Song, D.; Peng, B. Functional fatigue behavior of NiTi-Cu dissimilar laser welds. *Mater. Des.* **2017**, *114*, 282–287. [CrossRef]
15. Senkevich, K.S.; Knyazev, M.I.; Runova, Y.E.; Shlyapin, S.D. Special Features of Formation of a TiNi—VT6 Diffusion Joint. *Met. Sci. Heat Treat.* **2013**, *55*, 419–422. [CrossRef]
16. Rehman, A.U.; Babu, N.K.; Talari, M.K.; Usmani, Y.S.; Al-Khalefah, H. Microstructure and mechanical properties of dissimilar friction welding Ti-6Al-4V alloy to Nitinol. *Metals* **2021**, *11*, 109. [CrossRef]
17. Zhou, X.; Chen, Y.; Huang, Y.; Mao, Y.; Yu, Y. Effects of niobium addition on the microstructure and mechanical properties of laser-welded joints of NiTiNb and Ti6Al4V alloy. *J. Alloys Compd.* **2018**, *735*, 2616–2624. [CrossRef]
18. Zhan, Z.; Chen, Y.; Wang, S.; Huang, Y.; Mao, Y. Prevention of crack formation in electron-beam welded joints of dissimilar metal compounds (TiNi/Ti-6Al-4V). *Met. Sci. Heat Treat.* **2019**, *61*, 373–378. [CrossRef]
19. Homma, T.; Takano, H.; Ozaki, T. Nanostructural analysis of welded Ti–6Al–4V by linear friction welding applied for blisk assemblies. *Materialia* **2019**, *5*, 100174. [CrossRef]

20. Vairis, A.; Frost, M. High frequency linear friction welding of a titanium alloy. *Wear* **1998**, *217*, 117–131. [CrossRef]
21. Chan, C.W.; Man, H.C.; Yue, T.M. Effect of postweld heat treatment on the microstructure and cyclic deformation behavior of laser-welded NiTi-shape memory wires. *Metall. Mater. Trans. A* **2012**, *43*, 1956–1965. [CrossRef]
22. Yan, X.J.; Yang, D.Z.; Liu, X.P. Influence of heat treatment on the fatigue life of a laser-welded NiTi alloy wire. *Mater. Characterisation* **2007**, *58*, 262–266. [CrossRef]
23. Geng, P.; Qin, G.; Ma, H.; Zhou, J.; Zhang, C.; Ma, N. Numerical modelling on the plastic flow and interfacial self-cleaning in linear friction welding of superalloys. *J. Mater. Process. Technol.* **2021**, *296*, 117198. [CrossRef]
24. Muralimohan, C.H.; Muthupandi, V.; Sivaprasad, K. Properties of Friction Welding Titanium-stainless Steel Joints with a Nickel Interlayer. *Procedia Mater. Sci.* **2014**, *5*, 1120–1129. [CrossRef]
25. Mishra, R.S.; Ma, Z.Y. Friction stir welding and processing. *Mater. Sci. Eng. R Rep.* **2005**, *50*, 1–78. [CrossRef]
26. Senkevich, K.S.; Shlyapin, S.D. Investigation of the process of diffusion bonding of alloys based on titanium nickelide. *Weld. Int.* **2012**, *26*, 736–738. [CrossRef]
27. Gotawala, N.; Shrivastava, A. Investigation of interface microstructure and mechanical properties of rotatory friction welded dissimilar aluminum-steel joints. *Mater. Sci. Eng. A* **2021**, *825*, 141900. [CrossRef]
28. Kumar, A.S.; Khadeer, S.A.; Rajinikanth, V.; Pahari, S.; Kumar, B.R. Evaluation of bond interface characteristics of rotary friction welded carbon steel to low alloy steel pipe joints. *Mater. Sci. Eng. A* **2021**, *824*, 141844. [CrossRef]
29. Ji, S.; Wang, Y.; Liu, J.; Meng, X.; Tao, J.; Zhang, T. Effects of welding parameters on material flow behavior during linear friction welding of Ti6Al4V titanium alloy by numerical investigation. *Int. J. Adv. Manuf. Technol.* **2016**, *82*, 927–938. [CrossRef]
30. Miranda, R.M.; Assunção, E.; Silva, R.J.C.; Oliveira, J.P.; Quintino, L. Fiber laser welding of NiTi to Ti-6Al-4V. *Int. J. Adv. Manuf. Technol.* **2015**, *81*, 1533–1538. [CrossRef]
31. Zoeram, A.S.; Mousavi, S.A. Laser welding of Ti–6Al–4V to Nitinol. *Mater. Des.* **2014**, *61*, 185–190. [CrossRef]
32. Deng, Y.; Sheng, G.; Xu, C. Evaluation of the microstructure and mechanical properties of diffusion bonded joints of titanium to stainless steel with a pure silver interlayer. *Mater. Des.* **2013**, *46*, 84–87. [CrossRef]